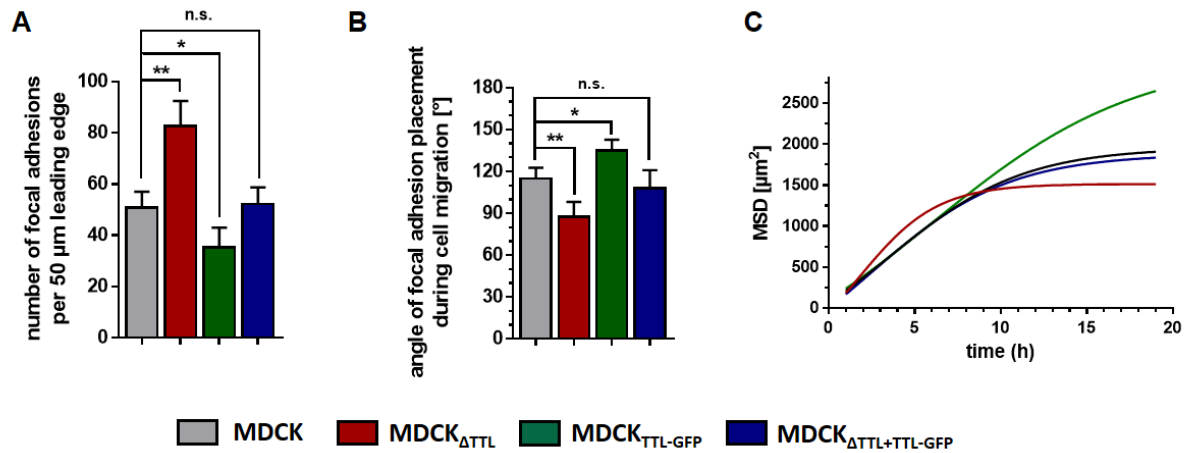


1 **Supplementary Material**

2

Figure S1

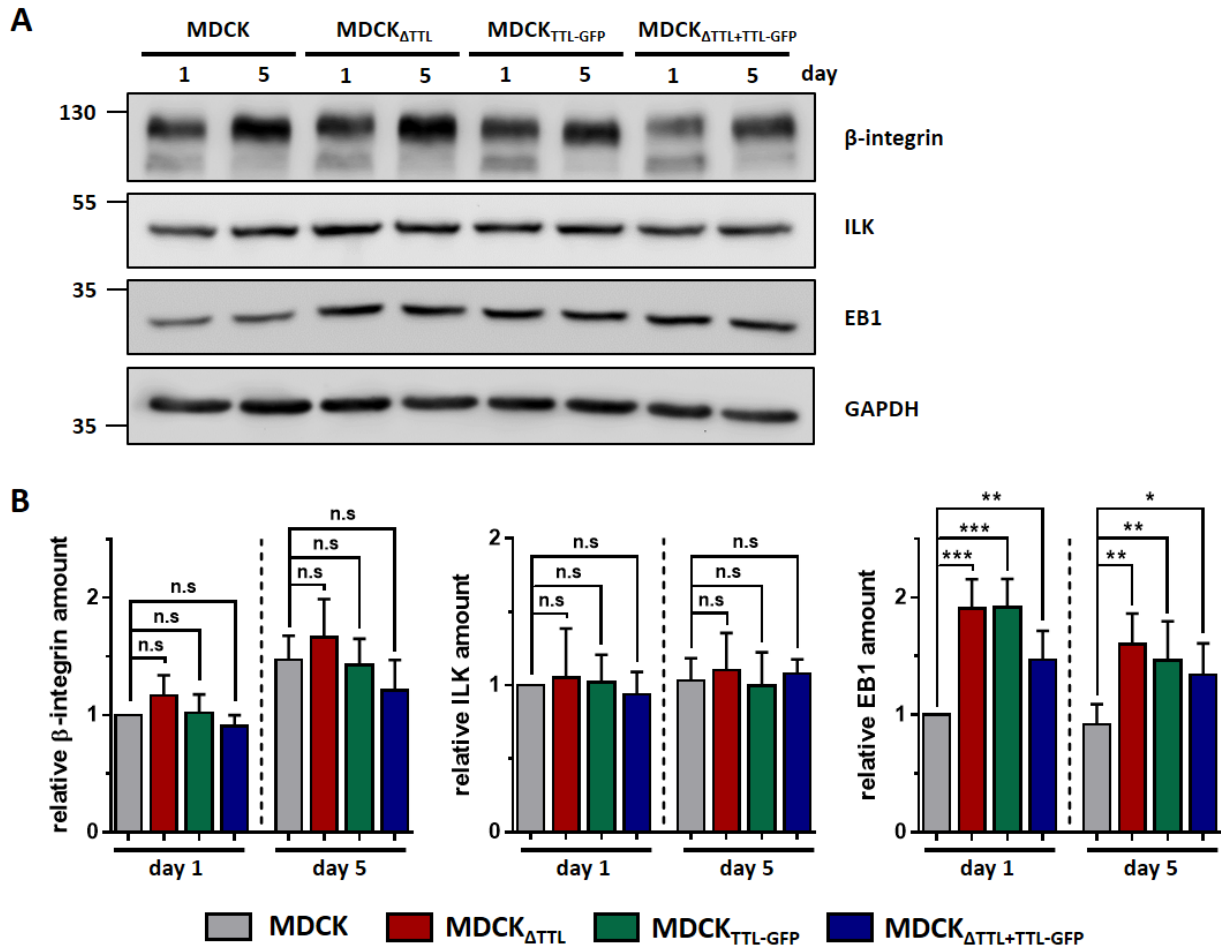


3

4 **Figure S1: Quantification of focal adhesions replacement during cell migration.**

5 (A) MDCK, MDCK<sub>ΔTTL</sub>, MDCK<sub>TTL-GFP</sub> and MDCK<sub>ΔTTL+TTL-GFP</sub> were stained after 6 h of migration as  
 6 described in figure 1. Number of focal adhesions per 50 μm leading edge were counted and quantified  
 7 for each cell line. Mean±s.d., n=3 independent experiments per cell line. Statistical significance was  
 8 tested using one-way ANOVA with Dunnet's comparison (n.s., not significant; \**P*<0.05; \*\**P*<0.01).  
 9 (B) Quantification of focal adhesion placement angle during cell migration in each cell line. Angles  
 10 were measured by ImageJ. A total of 10-15 cells were analyzed per experiment. Mean±s.d., n=3  
 11 independent experiments per cell line. Statistical significance was tested using one-way ANOVA with  
 12 Dunnet's comparison (n.s., not significant; \**P*<0.05; \*\**P*<0.01). (C) For MSD plots spline curves from  
 13 interpolated ImageJ tracking analysis of 4 cells per experiment were generated. n=6 independent  
 14 experiments per cell line.

Figure S2



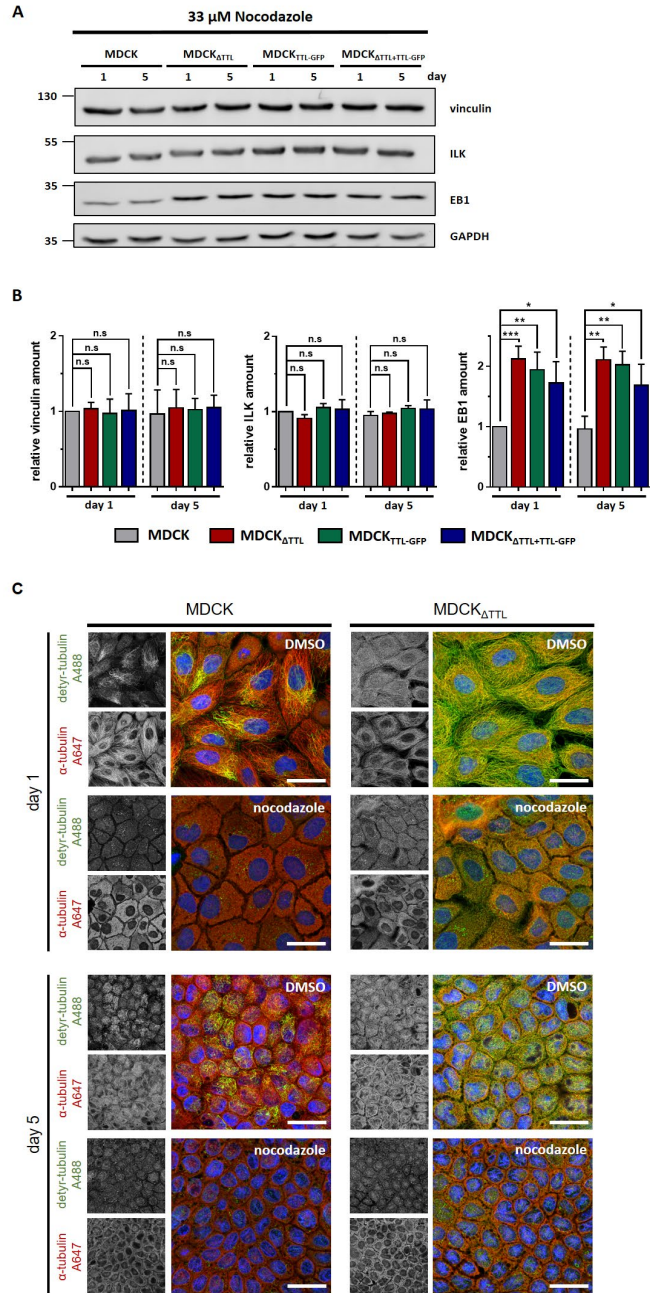
15

16 **Figure S2: Expression profiles of β1-integrin, ILK and EB1 in MDCK, MDCK<sub>ΔTTL</sub>, MDCK<sub>TTL-GFP</sub> and MDCK<sub>ΔTTL+TTL-GFP</sub> cells.**  
 17

18 (A, B) Lysates of subconfluent and confluent MDCK, MDCK<sub>ΔTTL</sub>, MDCK<sub>TTL-GFP</sub> and MDCK<sub>ΔTTL+TTL-GFP</sub>  
 19 GFP cells were analyzed by immunoblot with antibodies directed against β1-integrin (CD29), ILK and  
 20 EB1. Equal amounts (20 μg) of lysates were loaded. GAPDH served as a loading control.  
 21 Representative results. (B) Relative quantities were normalized to GAPDH levels in cell lysates.  
 22 Mean±s.d., n=3. Statistical significance was tested using one-way ANOVA with Dunnet's comparison  
 23 (n.s., not significant; \**P*<0.05; \*\**P*<0.01; \*\*\**P*<0.001).

24

Figure S3

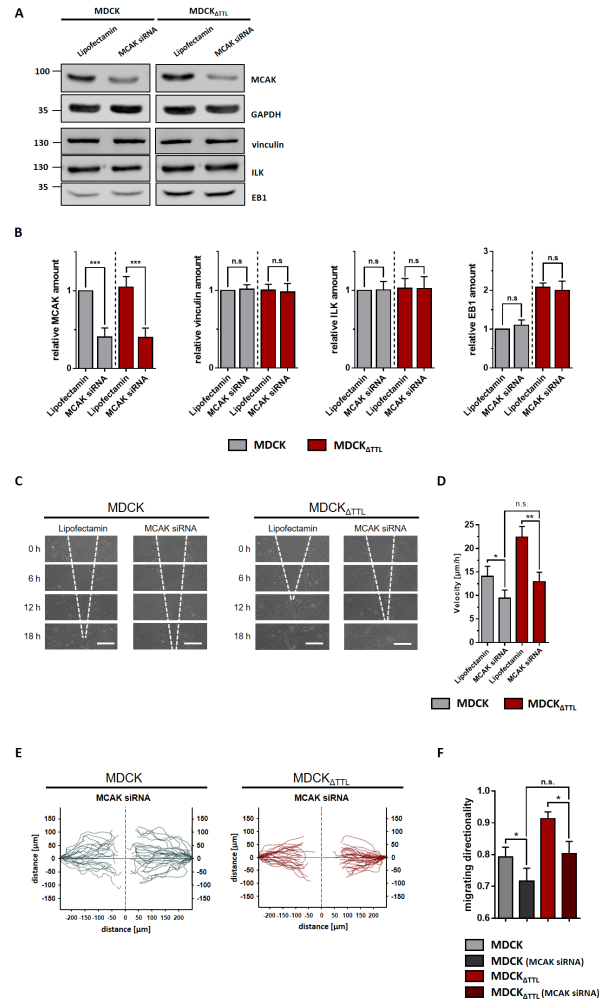


25

26 **Figure S3: Effect of nocodazole treatment on the expression patterns of vinculin, ILK and EB1.**

27 (A, B) Lysates of subconfluent and confluent MDCK, MDCK $\Delta$ TTL, MDCK $_{TTL-GFP}$  and MDCK $\Delta$ TTL+TTL-  
 28 GFP cells, treated with 33  $\mu$ M nocodazole for 1 h on ice and 1 h at 37°C, were analyzed by immunoblot  
 29 with antibodies directed against vinculin, ILK and EB1. Equal amounts of lysates were loaded.  
 30 GAPDH served as a loading control. Representative results. (B) Relative quantities were normalized  
 31 to GAPDH in cell lysates. Mean $\pm$ s.d., n=3. Statistical significance was tested using one-way ANOVA  
 32 with Dunnet's comparison (n.s., not significant; \* $P$ <0.05; \*\* $P$ <0.01; \*\*\* $P$ <0.001). (C) Successful  
 33 disruption of microtubules following nocodazole-treatment was analyzed in non-polarized and  
 34 polarized MDCK and MDCK $\Delta$ TTL cells. The cells were fixed and stained for  $\alpha$ -tubulin (red) and detyr-  
 35 tubulin (green). Scale bars: 30  $\mu$ m.

Figure S4

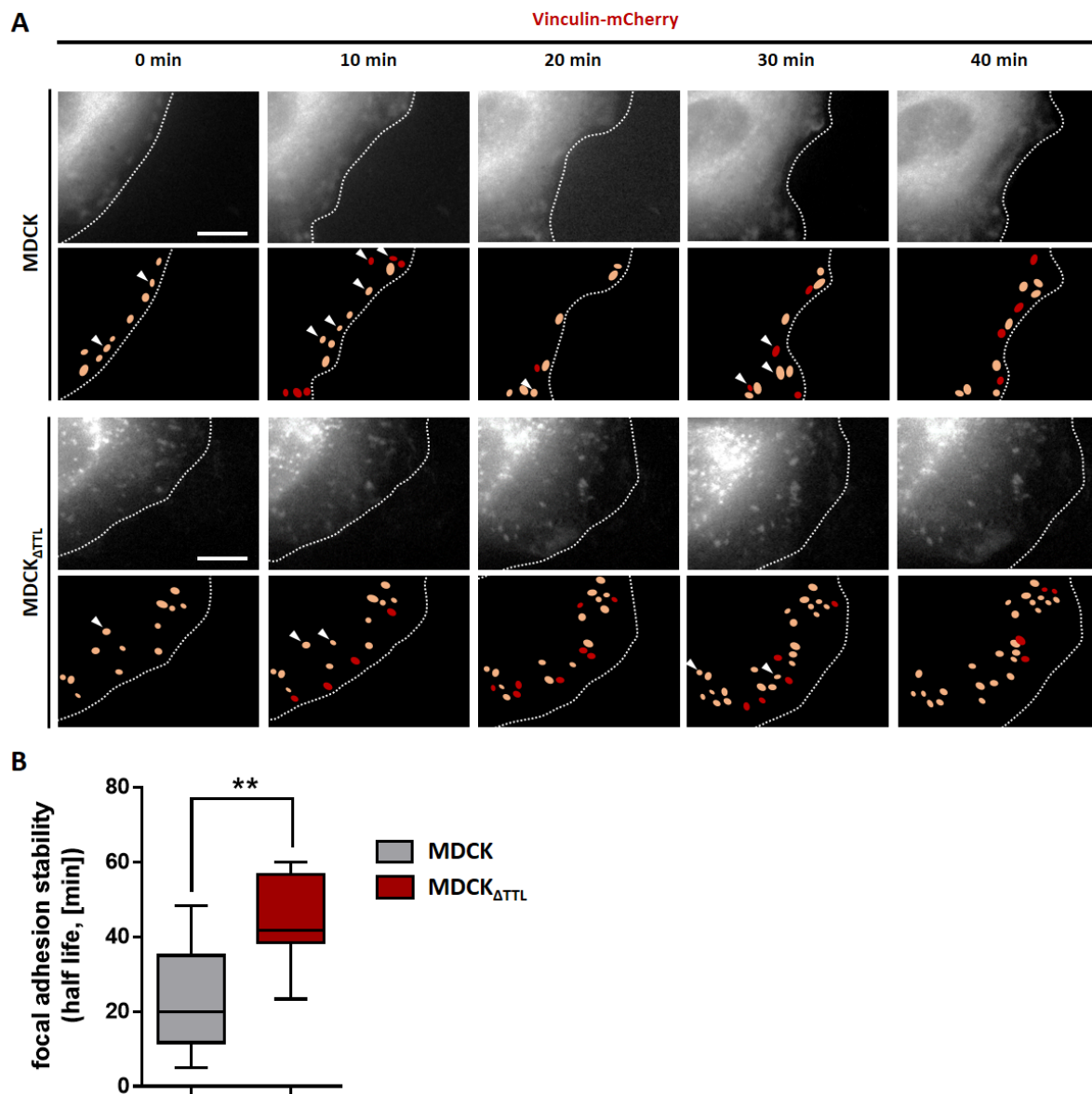


36

37 **Figure S4: MCAK-knockdown leads to delayed cell migration after TTL-modulation.**

38 (A) MDCK and MDCK $_{\Delta TTL}$  cells were transfected with MCAK-specific siRNA. Lysates of control  
 39 cells (lipofectamin treated) and MCAK-depleted cells were analyzed by immunoblot with antibodies  
 40 directed against MCAK, vinculin, ILK and EB1. GAPDH served as a loading control. n=3 independent  
 41 experiments. Representative result. (B) Relative quantities were normalized to GAPDH levels in cell  
 42 lysates. Mean $\pm$ s.d., n=3. Statistical significance was tested using one-way ANOVA with Dunnet's  
 43 comparison (n.s., not significant; \*\*\* $P$ <0.001). (C) Confluent MDCK and MDCK $_{\Delta TTL}$  cell-monolayers  
 44 of MCAK-depleted and control cells (lipofectamin treated) were scratch wounded to analyze wound  
 45 closure. Cells were recorded at 0, 6, 12 and 18 h post-scratching. White dotted lines indicate the wound  
 46 borders progress. Scale bars: 100  $\mu\text{m}$ . (D) Mean cell migration velocity was calculated. Mean $\pm$ s.d.,  
 47 n=3. Statistical significance was tested using one-way ANOVA with Dunnet's comparison (n.s., not  
 48 significant; \* $P$ <0.05; \*\* $P$ <0.01). (E) Single cell migration was recorded and visualized by Tracking  
 49 Tool<sup>TM</sup> PRO (Gradientech). One line corresponds to one single cell track of each cell line. (F) Cell  
 50 migration directionality was calculated by Tracking Tool<sup>TM</sup> PRO. Mean $\pm$ s.d., n=3 independent  
 51 experiments per cell line were performed. Statistical significance was tested using one-way ANOVA  
 52 with Dunnet's comparison (n.s., not significant; \* $P$ <0.05).

Figure S5

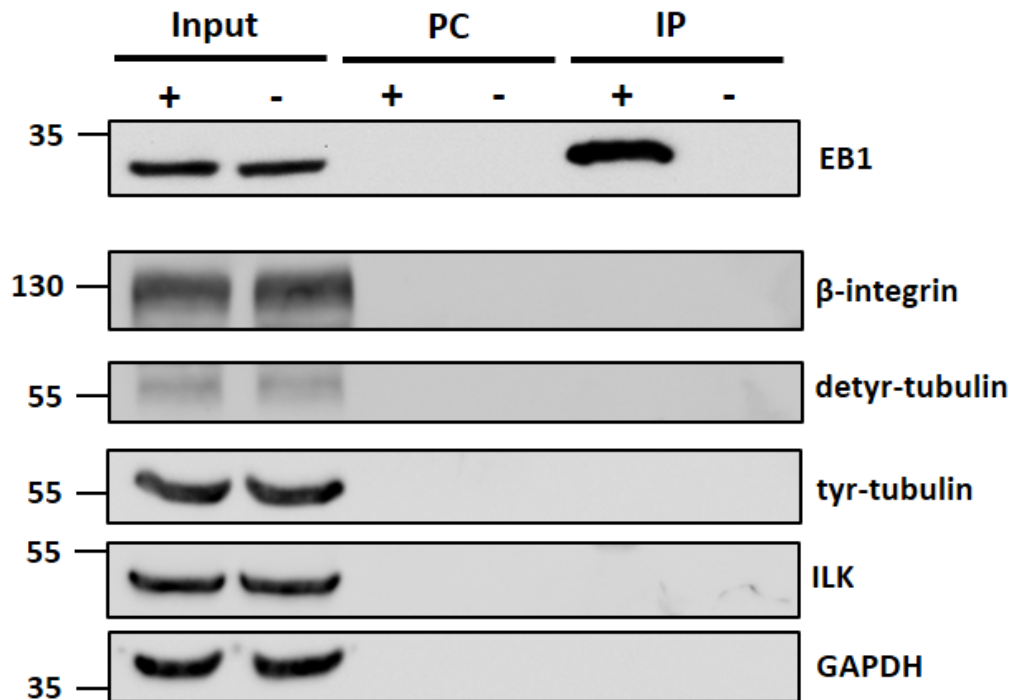


53

54 **Figure S5: Stability of vinculin-mCherry labelled FAs in MDCK cells.**

55 (A) Migrating MDCK and MDCK $\Delta$ TTL cells transiently transfected with vinculin-mCherry incubated  
56 on glass bottom WillCo dishes under a humidified atmosphere of 5% CO<sub>2</sub> in air. Assembly and  
57 disassembly of focal adhesions were analyzed by fluorescence microscopy at 37 °C. Vinculin-mCherry  
58 fluorescence after varying time intervals is indicated in the upper rows and identified FAs are depicted  
59 in the lower rows. Newly formed FAs per time interval are shown in red, FAs fading away in one time  
60 interval are indicated by arrowheads, remaining FAs are labelled in orange. White dotted lines indicate  
61 the migration progress. Scale bars, 10  $\mu$ m. (B) Quantification of FAs half-lives in MDCK and  
62 MDCK $\Delta$ TTL cells. Mean $\pm$ s.d., n=3. Statistical significance was tested with Student's unpaired t-test  
63 (\*\*P<0.01).

## Figure S6



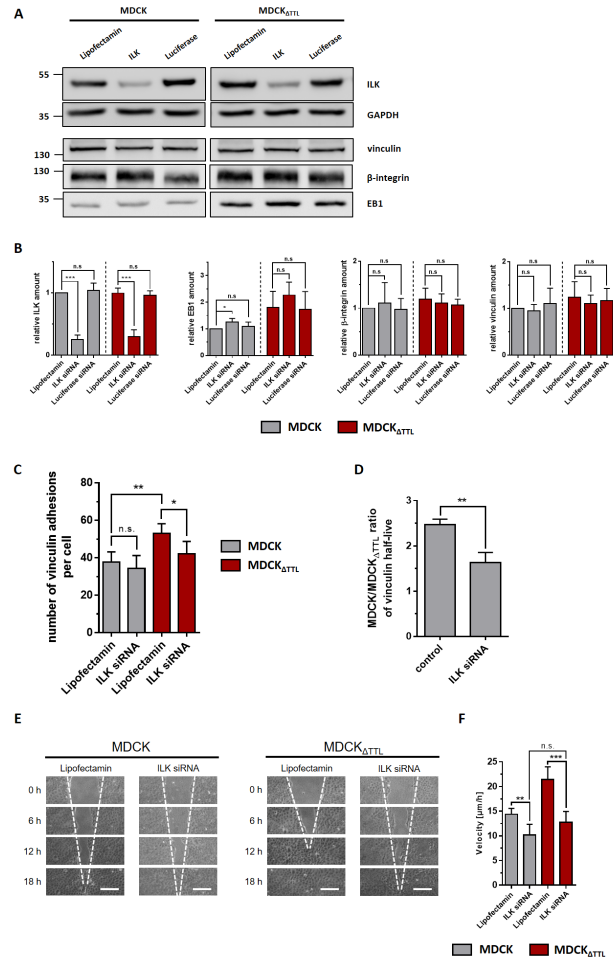
64

65 **Figure S6: TTL-overexpression reduces pulldown of EB1 with tubulin and ILK.**

66 MDCK<sub>TTL-GFP</sub> cell lysates were incubated with anti-EB1 antibodies followed by precipitation with  
67 agarose beads. Precipitates were analyzed by immunoblot using antibodies directed against  $\beta$ 1-integrin,  
68 detyr-tubulin, tyr-tubulin, ILK, GAPDH and EB1. Representative results, n=3 independent  
69 experiments. PC, Pre-clearing using agarose beads; IP+, Immunoprecipitation using EB1 antibodies  
70 and agarose beads; IP-, Immunoprecipitation using unspecific IgG antibodies and agarose beads.

71

Figure S7



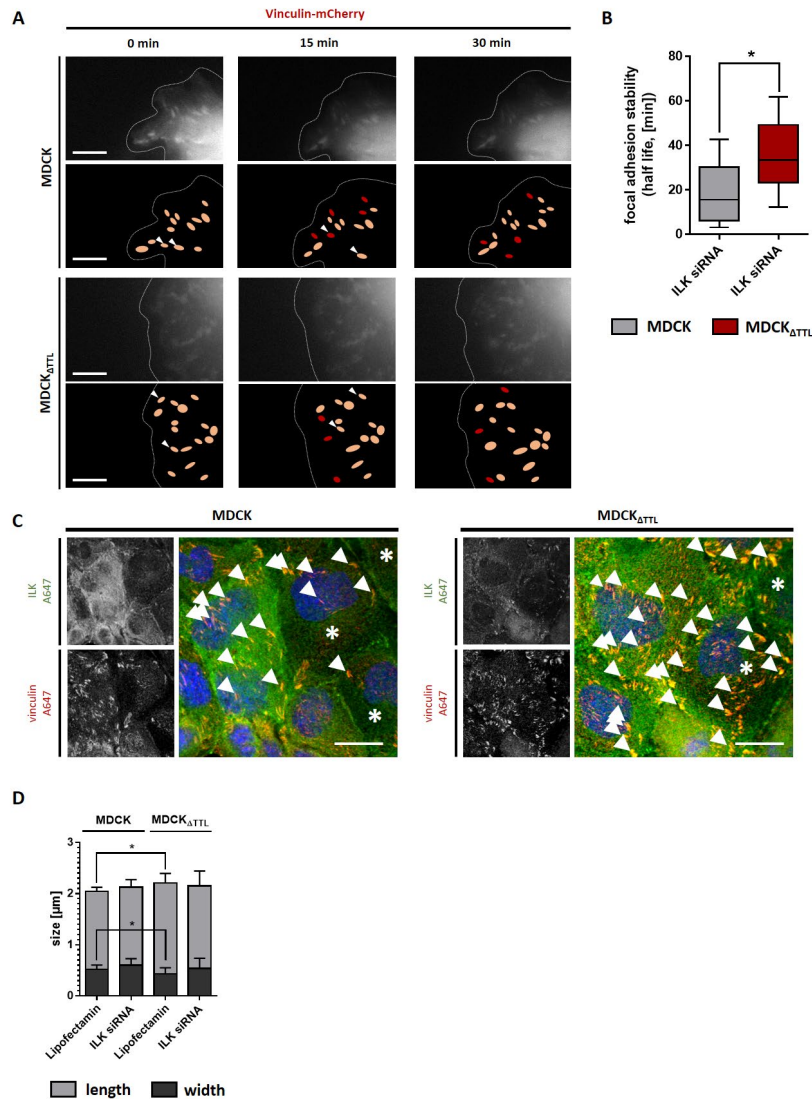
72

73 **Figure S7: ILK-knockdown delays cell migration and reduces focal adhesion quantities after**  
 74 **TTL-modulation.**

75 (A) MDCK and MDCK<sub>ΔTTL</sub> cells were transfected with ILK-specific siRNA overnight. Lysates of  
 76 control cells (lipofectamin treated), ILK-depleted cells and luciferase-siRNA treated cells were  
 77 analyzed by immunoblot with antibodies directed against integrin linked kinase (ILK), vinculin,  
 78 β1-integrin (CD29) and EB1. Equal amounts (20 μg) of lysates were loaded. GAPDH served as a loading  
 79 control. n = 3 independent experiments. Representative result. (B) Relative quantities were normalized  
 80 to GAPDH levels in cell lysates. Mean±s.d., n=3. Statistical significance was tested using one-way  
 81 ANOVA with Dunnet's comparison (n.s., not significant; \*P<0.05; \*\*\*P<0.001). (C) Quantification  
 82 of vinculin-positive focal adhesions per cell. Comparison of cells after knockdown of ILK and control  
 83 cells (lipofectamin treated). Mean±s.d., 8 – 10 cells per experiment, n=3 independent experiments.  
 84 Statistical significance was tested using one-way ANOVA with Dunnet's comparison (n.s., not  
 85 significant; \*P<0.05; \*\*P<0.01). (D) Quantification of MDCK/MDCK<sub>ΔTTL</sub> vinculin half-life ratio.  
 86 Mean±s.d., n=3. Statistical significance was tested with Student's unpaired t-test (\*\*P<0.01). (E)  
 87 Confluent MDCK and MDCK<sub>ΔTTL</sub> cell-monolayers of ILK-depleted and control cells (lipofectamin  
 88 treated) were scratch wounded to analyze migration velocity. Cells were recorded at 0, 6, 12 and 18 h  
 89 post-scratching. White dotted lines indicate the wound borders progress. Scale bars: 100 μm. (F) Mean  
 90 cell migration velocity was calculated. Mean±s.d., n=5. Statistical significance was tested using one-  
 91 way ANOVA with Dunnet's comparison (n.s., not significant; \*\*P<0.01; \*\*\*P<0.001).



Figure S8



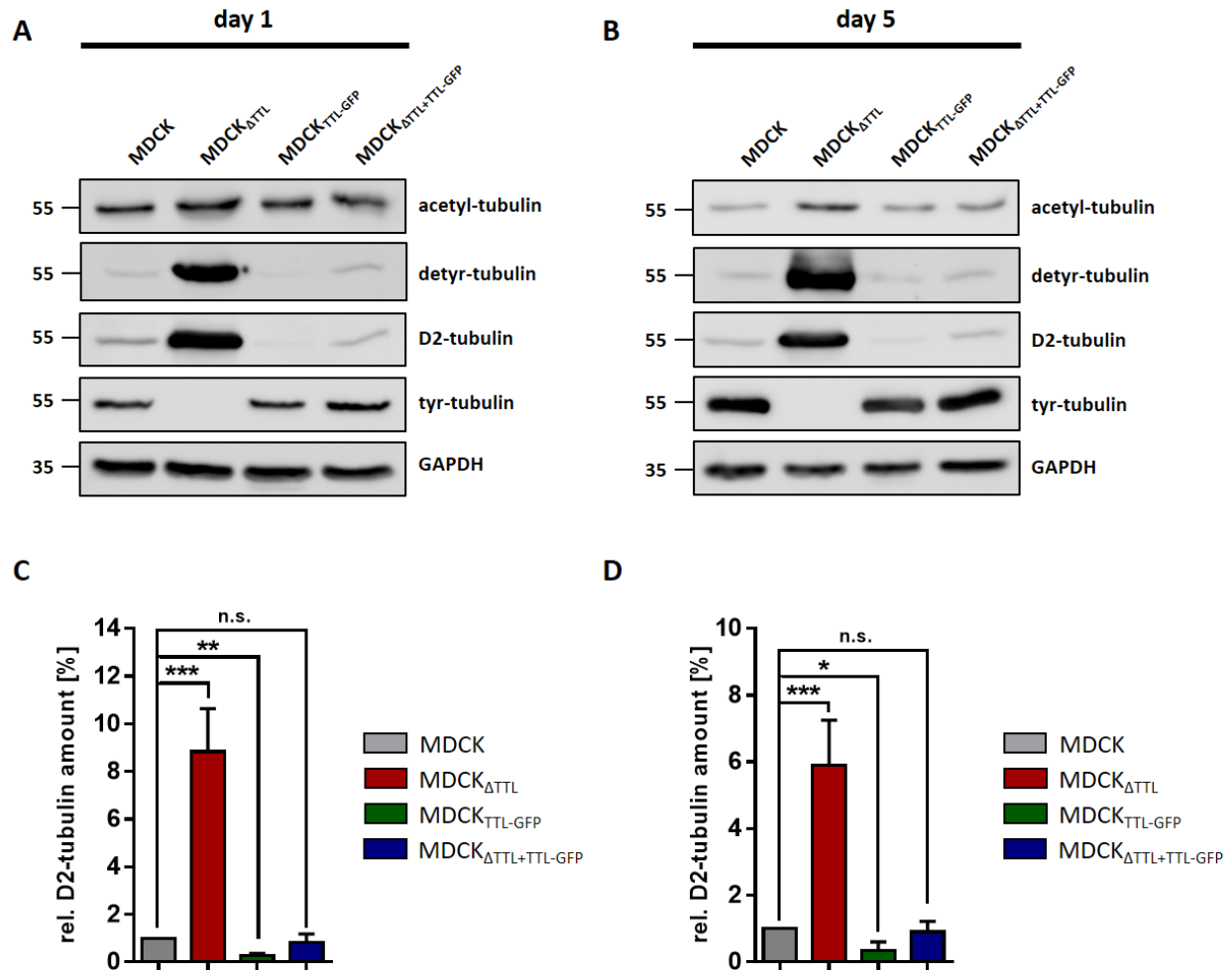
92

93 **Figure S8: ILK-knockout changes dynamic and size of focal adhesions.**

94 (A) Migrating ILK-depleted MDCK and MDCK<sub>ΔTTL</sub> cells transiently transfected with vinculin-  
 95 mCherry were analyzed by fluorescence microscopy at 37 °C. Vinculin-mCherry fluorescence after  
 96 varying time intervals is indicated in the upper rows and identified FAs are depicted in the lower  
 97 rows. Newly formed FAs per time interval are shown in red, FAs fading away in one time interval are  
 98 indicated by arrowheads, remaining FAs are labelled in orange. White dotted lines indicate the  
 99 migration progress. Scale bars, 8 μm. (B) Quantification of FAs half-lives in MDCK and MDCK<sub>ΔTTL</sub>  
 100 cells. Mean±s.d., n=3. Statistical significance was tested with Student's unpaired t-test (\*P<0.05). (C)  
 101 ILK-depleted MDCK and MDCK<sub>ΔTTL</sub> cells were immunostained for ILK (green) and vinculin (red)  
 102 Scale bars: 10 μm. Arrowheads indicate exemplary vinculin spots. Asterisks indicate cells with down  
 103 knocked ILK. (D) Quantification of FAs (vinculin) length (light grey) and width (dark grey) in MDCK  
 104 and MDCK<sub>ΔTTL</sub> cells following ILK-knockdown by siRNA. Mean±s.d., n=3 independent experiments  
 105 per cell line. Statistical significance was tested using one-way ANOVA with Dunnet's comparison  
 106 (\*P<0.05).



Figure S9



108

109

110 **Figure S9: TTL knockout leads to increased amount of D2-tubulin.**

111 (A,B) Cellular levels of acetyl-tubulin, detyr-tubulin, D2-tubulin and tyr-tubulin were assessed by  
 112 Western blot analysis of cell lysates from non-polarized (A) and polarized (B) MDCK, MDCK $_{\Delta TTL}$ ,  
 113 MDCK $_{TTL-GFP}$ , and MDCK $_{\Delta TTL+TTL-GFP}$  cells. Protein concentrations of the lysates were determined and  
 114 equal amounts were loaded on each lane of the SDS-PAGE. Representative results. (C,D)  
 115 Quantification of relative D2-tubulin expression in each cell line as compared to MDCK cells for non-  
 116 polarized (C) and polarized (D) cells. Relative polypeptide expressions were normalized to GAPDH  
 117 levels. Quantities from MDCK cells were set as 1. Mean $\pm$ s.d.,  $n=3$ . Statistical significance was tested  
 118 using one-way ANOVA with Dunnet's comparison (n.s., not significant; \* $P < 0.05$ ; \*\* $P < 0.01$ ;  
 119 \*\*\* $P < 0.001$ ).

120

121 **Movie S10: EB1-dynamics in MDCK.**

122 Subconfluent living MDCK cells transiently transfected with EB1-GFP incubated on glass bottom  
123 WillCo dishes under a humidified atmosphere of 5% CO<sub>2</sub> in air. Dynamic of EB1-GFP (grey) was  
124 analyzed by fluorescence microscopy at 37 °C. Time-lapse imaging was recorded for 60 sec. Scale bar:  
125 5 μm.

126 **Movie S11: EB1-dynamics in MDCK<sub>ΔTTL</sub>.**

127 Subconfluent living MDCK<sub>ΔTTL</sub> cells transiently transfected with EB1-GFP incubated on glass bottom  
128 WillCo dishes under a humidified atmosphere of 5% CO<sub>2</sub> in air. Dynamic of EB1-GFP (grey) was  
129 analyzed by fluorescence microscopy at 37 °C. Time-lapse imaging was recorded for 60 sec. Scale bar:  
130 5 μm.

131 **Movie S12: Basal and apical dynamics of EB1 in MDCK cysts.**

132 Living MDCK cells stably transfected with EB1-GFP were cultured in Matrigel for 7 days. Dynamics  
133 of EB1-GFP (grey) was analyzed by fluorescence microscopy at 37 °C and a humidified atmosphere  
134 of 5% CO<sub>2</sub> in air. Time-lapse imaging was recorded for 51 sec. Each arrow indicates EB1-GFP comet-  
135 like movement orientated to the apical membrane. Scale bar: 20 μm.

136 **Movie S13: Basal and apical dynamics of EB1 in MDCK<sub>ΔTTL</sub> cysts.**

137 Living MDCK<sub>ΔTTL</sub> cells stably transfected with EB1-GFP were cultured in Matrigel for 7 days.  
138 Dynamics of EB1-GFP (grey) was analyzed by fluorescence microscopy at 37 °C and a humidified  
139 atmosphere of 5% CO<sub>2</sub> in air. Time-lapse imaging was recorded for 63 sec. Arrow indicates EB1-GFP  
140 comet-like movement orientated to the apical membrane. Scale bar: 20 μm.

**Table 1**

	MDCK	MDCK <sub>ΔTTL</sub>	MDCK <sub>TTL-GFP</sub>	MDCK <sub>ΔTTL+TTL-GFP</sub>
n	velocity	velocity	velocity	velocity
1	12,0	24,0	9,0	13,9
2	12,0	22,2	8,5	13,6
3	16,0	20,4	12,3	16,5
4	13,4	20,7	8,4	12,8
5	13,4	23,9	7,3	16,5
6	14,3	24,4	11,0	12,7
<b>mean</b>	<b>13,52</b>	<b>22,60</b>	<b>9,42</b>	<b>14,33</b>
<b>SD</b>	<b>± 1,38</b>	<b>± 1,61</b>	<b>± 1,70</b>	<b>± 1,59</b>

142

143 **Table 1: Migration velocity in wound healing assay.**

144 Migration velocity [ $\mu\text{m}/\text{h}$ ] of MDCK, MDCK<sub>ΔTTL</sub>, MDCK<sub>TTL-GFP</sub> and MDCK<sub>ΔTTL+TTL-GFP</sub>. Cells were  
 145 incubated on a glass bottom Wilco Dish to form a confluent monolayer. Scratches were added by sterile  
 146 micropipette tip. Cell migration experiments were recorded on a PAULA microscope (Personal  
 147 Automated Lab Assistant, Leica Microsystems). Scratch closure rates were recorded to deduce  
 148 migration velocities by monolayer edge velocimetry (ImageJ analysis tools). n=6. SD=standard  
 149 deviation.